ACS OMEGA

Open Access

http://pubs.acs.org/journal/acsodf

Article

"Allergolds": Gold Nanocluster-Based Bioconjugates of Food Allergens with Reduced Immunoglobulin E Binding

Victor Martinez-Macias, Scott A. Gabel, J. Craig Bennett, Scott A. Smith, Geoffrey A. Mueller, Geniece L. Hallett-Tapley,[§] and Alexander C.Y. Foo*[,§]

Cite This: *ACS Omega* 2025, 10, 9040−9050

Read Online

ACCESS | Metrics & More | Article Recommendations | Supporting Information

ABSTRACT: Allergen-specific immunotherapy represents the only method of achieving a lasting reduction in the severity of allergic symptoms. However, the need to expose patients to the allergens to which they are sensitized carries risks. One solution is to use denatured allergens whereby the structure of allergenic proteins is disrupted, preventing their recognition by immunoglobulin E (IgE) antibodies and thus reducing the risk of adverse reactions. Denaturation is often carried out by using chemical cross-linking to generate allergoids. Gold nanoclusters (AuNCs) are emerging as versatile tools in biotechnology due in part to their ability to conjugate a wide range of biological molecules. Previous works have described the formation of AuNC using egg allergens such as Gal d 4 (lysozyme), Gal d 2 (ovalbumin), and whole egg whites. In all cases, AuNC bioconjugation disrupted the protein structure, allowing for their use in biosensing applications. In this work, we hypothesize that these AuNC-allergen bioconjugates could be used to generate "Allergolds", chemically altered versions of allergenic proteins analogous to traditional allergoid formulations. Using spectroscopic techniques, we confirm that the formation of AuNC bioconjugates of the chicken egg Gal d 4 and Gal d 2 disrupts protein structure when generated from both purified protein and whole egg whites. This structural perturbation was found to be resilient to a range of chemical conditions and successfully disrupted recognition by human IgE. These results establish Allergolds as a potential tool for generating systematically denatured allergens from both purified proteins and biological extracts.

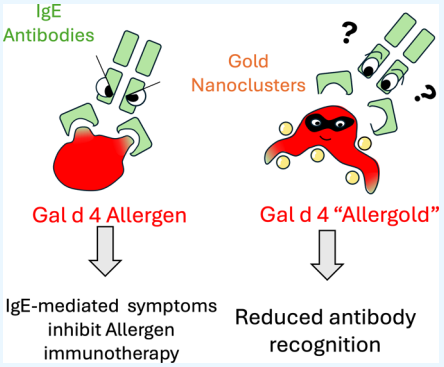

INTRODUCTION

Food allergy is a major health concern that currently affects up to 10% of children and 3% of adults: a prevalence that has been steadily increasing over the past decades. This surge in food allergies has paralleled an uptick in cases of food-induced anaphylaxis.[1,2] An estimated 40% of children with a food allergy have experienced at least one anaphylactic episode.[3] The threat of such life-threatening reactions can contribute to anxiety, eating disorders,[4] and other sociological issues, further increasing the impact of food allergies on physical, mental, and socioeconomic wellbeing.[5]

The use of antihistamines, corticosteroids, and epinephrine to address acute symptoms following allergen exposure is well established; however, curative options to reduce reactivity and prevent symptoms are limited to allergen immunotherapy (AIT).[6] The adverse reactions experienced by allergic patients upon exposure to allergens (either inadvertently or via AIT) are mediated by immunoglobulin E (IgE) antibodies, which bind to specific epitopes on the allergen surface to trigger an immune response. AIT aims to "retrain" the immune system through controlled exposure to the sensitizing agent(s). Here, allergenic extracts are administered to patients over a prolonged time. This exposure regime encourages the production of "blocking" IgG antibodies, which compete with IgE for binding to the allergen upon exposure, reducing or eliminating the symptoms of allergic sensitization. While effective, exposing patients to the very same substances to which they are sensitized introduces the risk of adverse reactions.[7,8] This risk can be alleviated through limiting the doses administered or altering the route of exposure, but at the cost of reducing the effectiveness of treatment.[9]

One solution is to use allergoids. Here, allergens are chemically modified in a manner that disrupts its 3D structure. This inhibits antibody recognition, reducing the severity of IgE-mediated side effects upon exposure.[10−12] While the exact mechanism for the therapeutic benefit of allergoid-mediated AIT remains a topic of discussion, the use of allergoids derived from denatured allergenic proteins has been proven to be effective in a clinical setting.[13,14] Historically, allergoids are generated using nonspecific chemical cross-linkers. Common agents include formaldehyde or glutaraldehyde, although

Received: August 15, 2024
Revised: February 7, 2025
Accepted: February 13, 2025
Published: February 28, 2025

various alternatives have been proposed.[15] A less common approach is to employ physical denaturants, such as heat or pH, to generate denatured versions of allergenic proteins. The nonspecific nature of these approaches provides a versatile and economic avenue to generate AIT agents. However, the resulting product is often heterogeneous in nature, making it difficult to precisely monitor its composition or control dosage.[16−18] Physical denaturants such as heat or acid also have the additional problems of stability, with the protein eventually refolding into its native state over time. Recent works have attempted to address these issues by generating hypoallergens: genetically engineered versions of allergenic proteins in which the IgE epitopes have been specifically disrupted. This strategy has been used successfully to generate high-purity, samples of peanut[19] and egg[20] allergens with well-defined immunogenic properties. However, such an approach requires a detailed structural characterization of the major IgE-binding epitopes of the allergen in question. The requirement to express these hypoallergens using recombinant organisms also increases production complexity, further limiting their viability for widespread and cost-effective treatment options.

Nanotechnology may provide a viable compromise between heterogeneous allergoids and bespoke, genetically engineered hypoallergens. Recently, gold nanoclusters (AuNC) have received considerable interest due to their ability to conjugate a wide range of proteins, including the egg allergens Gal d 4 and Gal d 2. These bioconjugates can be easily generated from both purified proteins and whole extracts by using mild conditions. Bioconjugation is mediated by disulfide bonds between cysteine residues on the allergenic proteins and the metallic gold nanoclusters,[21,22] though the exact mechanism through which this occurs is not fully understood. Most proteins (including Gal d 4 and Gal d 2) include several buried cysteine residues that participate in covalent disulfide bonds that are instrumental in maintaining protein folding. Formation of Au−S bonds disrupts these interactions, altering the protein's structure.[21,23] The resulting AuNC bioconjugates are extremely well-defined with good biocompatibility and consistent particle morphology, combining the advantages of both traditional allergoids and hypoallergenic proteins while being relatively easy to synthesize. Despite this, the potential for AuNC bioconjugates in this application is yet to be explored.

In the present work, we explore whether AuNC bioconjugates can be used as an effective tool to generate persistently denatured allergens or "Allergolds" from hen egg white lysozyme, a major food allergen (WHO/IUIS designation: Gal d 4). Using established protocols, AuNC-Gal d 4 bioconjugates were generated from both purified protein and whole egg whites.[24,25] Loss of protein structure and function was confirmed using intrinsic tryptophan fluorescence, circular dichroism (CD), and enzymatic assays.[21] The resulting conjugates were extremely stable, being able to sustain Gal d 4 in its altered conformation for several months, and showed resistance against high-temperature conditions and dehydration. This contrasts with thermally denatured Gal d 4, which regained its structure and function within the span of an hour. Using competition ELISA assays, we show that the irreversible loss of structure and function upon conjugation completely abolished recognition by human IgE derived from allergic patient sera. Finally, we demonstrate the potential versatility of this approach by generating Allergolds using other food allergens from hen egg whites (Gal d 2). Lysozyme-AuNC bioconjugates have been extensively examined for a variety of biotechnology applications. The ability to generate AuNC-bioconjugates with reduced IgE binding using unaltered (native) food allergen proteins with minimal preparation establishes Allergolds as a viable alternative to both traditional allergoid preparations and genetically modified hypoallergens.

MATERIALS AND METHODS

Materials. Tetrachloroauric acid trihydrate ($HAuCl_4 \cdot 3H_2O$) and lysozyme (lyophilized powder from chicken egg white) were purchased from MilliporeSigma Canada and used as received. Sodium hydroxide and all other chemicals were obtained from Fisher Scientific Canada. The chicken lysozyme ELISA kit (colorimetric) NBP2-60088 was purchased from NOVUS Biologicals. The enzyme lysozyme activity assay kit E22013 was obtained from Invitrogen. Sodium dodecyl sulfate (SDS) was purchased from EMD Millipore. 35% HCT sheep red blood cells (RBC) were obtained from Fisher Scientific. The high-purity water used throughout all experiments and collected from triply deionized water (TDW) was purified by a Milli-Q system with a resistivity of 18.2 MΩ cm at 25 °C.

Synthesis of AuNC. The protocol for lysozyme-gold nanocluster (AuNC-Gal d 4) synthesis was adapted from the work of Hui Wei and collegues:[25] In brief, equal volumes of 4 mM $HAuCl_4$ and 10 mg/mL of Gal d 4 in TDW were combined in a 15 mL centrifuge tube and vortexed for 5 min. One molar NaOH was added to the reaction mixture to a final concentration of 32 mM NaOH, and the resulting mixture was incubated at 37 °C for at least 8 h. Formation of AuNC was visually identified through the formation of a light orange-brown solution. A negative control was generated by incubating an equivalent concentration of lysozyme in 32 mM NaOH (pH 12.5) for >8 h in the absence of $HAuCl_4$.

Egg white-gold nanoclusters (AuNC-HEW) were synthesized by adapting the protocol of Joseph and Geckeler.[26] In brief, commercially available chicken egg white was freeze-dried to prepare an aqueous solution of 25 mg/mL. One milliliter of previous solution was mixed with 50 μL of 0.1 M $HAuCl_4$ and vortexed for 5 min. One molar NaOH was added for a final concentration of 0.16 M NaOH, and then, the solution was incubated at 37 °C for at least 8 h.

The synthesis of ovalbumin-gold nanoclusters (AuNC-Gal d 2) was done by adapting the previous protocol with changes in the incubation times and temperature reported by Li and colleagues.[27] In brief, equal volumes of 40 mg/mL of Gal d 2 and aqueous solution of 9.50 mM of $HAuCl_4$ were mixed under vigorous stirring at 30 °C for 5 min. One molar NaOH was added to the solution for a final concentration of 74 mM NaOH, and the mixture was incubated for 85 °C for 10 min while vigorously stirring. Formation of AuNC was visually identified through the formation of an orange-pink solution.

Data Presentation and Analysis. Values and uncertainties presented in this work represent the average and standard deviation of at least three trials representing three biological replicates and/or AuNC-purification batches, unless otherwise specified. Statistical significance was assessed using a student *t* test assuming unequal means.

Biophysical Characterization of AuNC. To confirm formation of AuNC-allergen complexes, the fluorescence spectrum of the product was measured from 400 to 700 nm (λ_{ex}: 360 nm) using a Varioskan LUX spectrophotometer. The size of the resulting particles was assessed via dynamic light scattering (DLS) using a Malvern Zeta Sizer DLS.

https://doi.org/10.1021/acsomega.4c07425
ACS Omega 2025, 10, 9040−9050

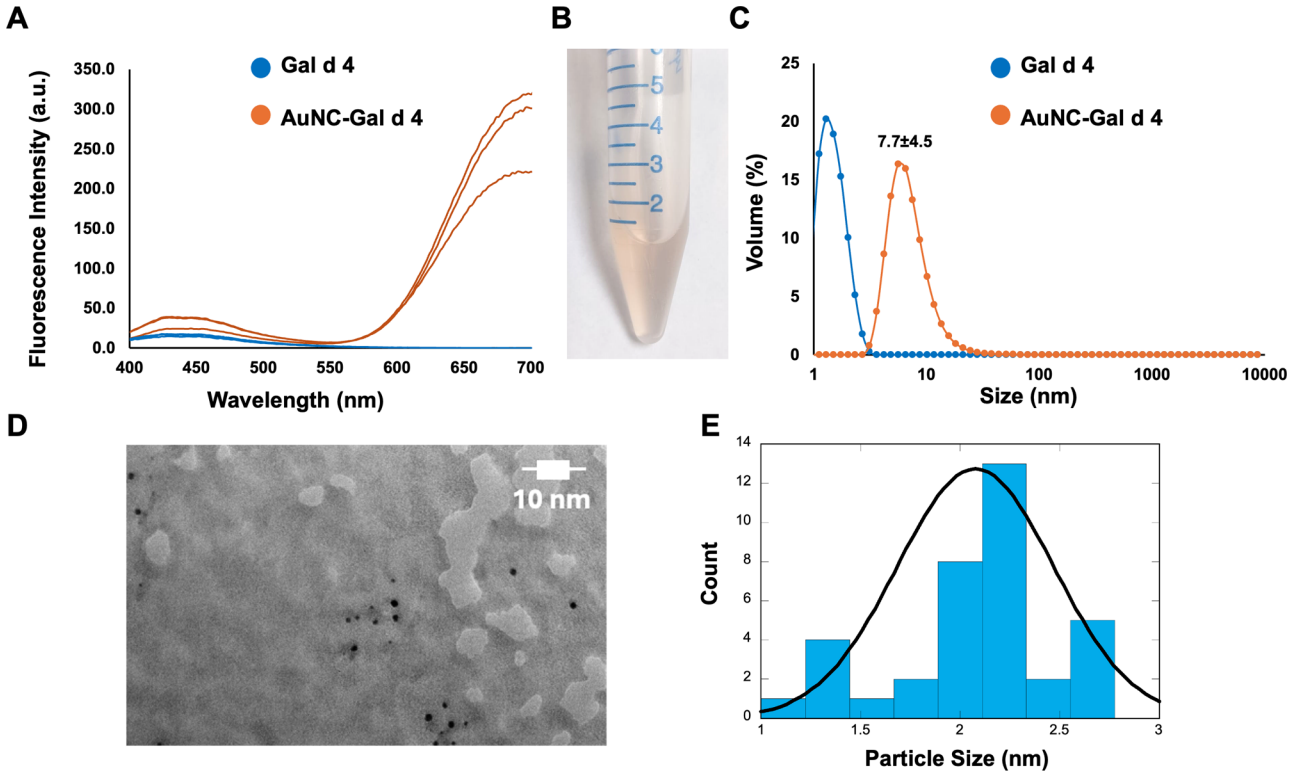

Figure 1. Formation of AuNC-Gal 4 nanoclusters. (A) Representative fluorescence spectra of AuNC-Gal d 4 (0.215 mM) showing the characteristic emission peak at 700 nm (λ_{ex}:360 nm). A control spectrum obtained from an equivalent concentration of unfunctionalized Gal d 4 is shown for comparison. Representative fluorescent spectra displayed here and elsewhere throughout the work are taken from three representative trials unless otherwise specified. Note that the three individual unfunctionalized Gal d 4 spectra cannot be distinguished due to overlap. (B) Representative image of Gal d 4 sample under visible light showing the characteristic orange color. (C) Average DLS size distribution per volume plot of prepared AuNC-Gal d 4 and Gal d 4, further confirming bioconjugate formation. (D) Representative TEM image of AuNC-Gal d 4. Additional images are available in Figures S1−S4. (E) Comparative size distribution analysis of the AuNC core size.

Additional characterization was carried out using size-exclusion chromatography via an Äkta Pure FPLC system (Cytiva). One milliliter of samples of AuNC-Gal d 4 (10 mg/mL) were loaded onto a Superdex 75 Increase 10/300 column equilibrated with water and eluted at 1 mL/min. Fractions (0.6 mL) were collected. Fractions corresponding to the main AuNC-Gal d 4 peak were collected and analyzed, as described above.

To evaluate the impact of AuNC formation on protein folding, tryptophan fluorescence of the bound protein was recorded from 300 to 600 nm (λ_{ex}: 280 nm). This was supported by circular dichroism (CD) measurements carried out using a Jasco J-815 CD Spectrometer. Measurements were performed using 1.5 μM Gal d 4 in TDW. To examine the effect of pH of lysozyme structure, samples of lysozyme were prepared in 20 m Tris buffer pH 3−12 and allowed to incubate for 2 h prior to measurement. Secondary structure estimations from the resulting spectra were obtained using the BeStSel (Beta Structure Selection) algorithm accessed via web server.[28,29]

Tryptophan fluorescence was used to monitor protein thermal stability between native Gal d 4 and AuNC-Gal d 4, and both samples were diluted in TDW with a final concentration of 50 μM. The assay was done by monitoring the fluorescence intensity at 340 nm with an excitation wavelength of 280 nm over a temperature ramp of 1 °C/min until reaching 90 °C using a Jasco FP-8250 spectrofluorometer.

Gal d 4 catalytic activity was measured using an Enzchek Lysozyme Assay kit (Invitrogen). Assays were carried out in accordance with the manufacturer-provided instructions. Here, the cleavage of an emissive substrate results in a fluorescence signal, which was measured over time using a Varioskan Lux spectrometer. All values were normalized relative to a control reaction carrier out using an equivalent concentration of undenatured Gal d 4 enzyme.

NMR data for Gal d 4 and AuNC-Gal d 4 in water (pH ∼ 7) were obtained by using a Bruker AVANCE II 400 MHz NMR spectrometer. ^{1}H NMR spectra with water suppression (Bruker pulse zgespg) were obtained at 25 °C. Spectra were normalized based on the number of scans and sample concentration.

TEM Characterization of AuNC-Gal d 4. Samples of AuNC-Gal d 4 were diluted with an equivalent volume of TDW. Ten microliters of the as-prepared AuNC sample was drop-casted onto a carbon coated grid and allowed to dry at room temperature. The sample was then analyzed with a Philips CM30 transmission electron microscope, operated at 250 kV acceleration voltage, equipped with a Gatan 832 OriusSC1000 CCD instrument using Digital Micrograph software. Average AuNC size was determined with ImageJ software by using a minimum of 30 measurements.

Immunological Characterization of AuNC-Gal d 4 and AuNC-HEW. The IgG antibody binding to AuNC-Gal d 4 and AuNC-HEW was assessed using commercially available ELISA kits (Novus). Assays were carried out in accordance with manufacturer instructions. Samples of the bioconjugates were

https://doi.org/10.1021/acsomega.4c07425
ACS Omega 2025, 10, 9040−9050

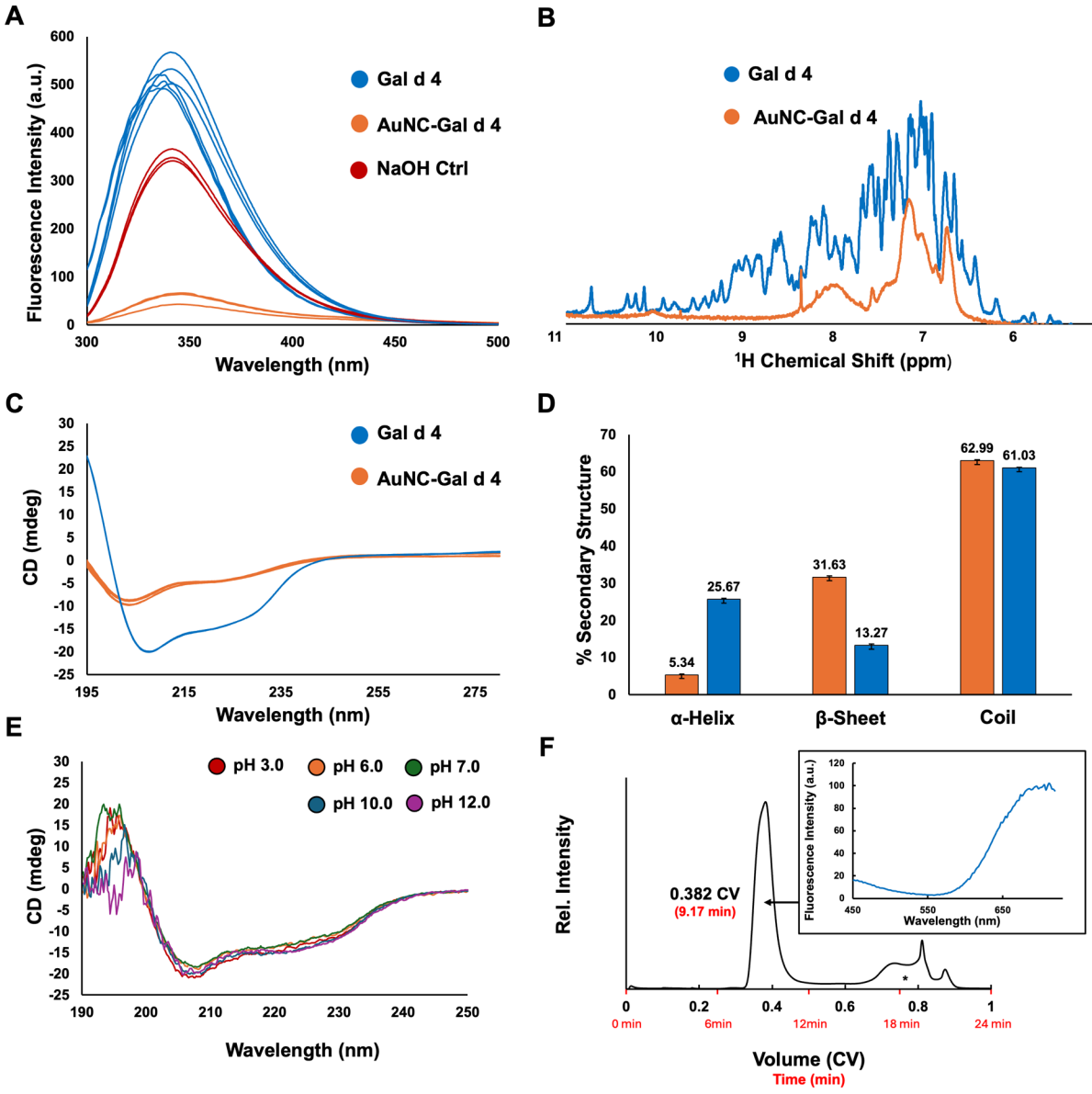

Figure 2. Conjugation with AuNC perturbs the Gal d 4 structure. (A) Representative tryptophan fluorescence spectra (λ_{ex}: 280 nm) of equivalent concentrations of Gal d 4, AuNC-Gal d 4, and the NaOH-treated negative control showing a loss of fluorescence intensity upon AuNC bioconjugation. (B) ^{1}H NMR spectra of Gal d 4 and AuNC-Gal d 4 showing the amide e ^{1}H region. Spectra were normalized for relative protein concentrations. (C) Representative CD spectra for equivalent concentrations of Gal d 4 and AuNC-Gal d 4, showing a loss of α-helical structure, represented by the peak intensity at 220 and 210 nm. Representative CD spectra are taken from at least three representative trials. Note that the individual Gal d 4 spectra cannot be distinguished due to overlap. (D) Quantification of secondary structure content from the CD spectra shown in panel (C) where orange bars correspond to the AuNC-Gal d 4 and blue bars correspond to the native Gal d 4. (E) CD spectra obtained for Gal d 4 (0.2 mg/mL) at various pH's. (F) Representative size-exclusion chromatography elution profile for AuNC-Gal d 4. A single peak is observed corresponding to the AuNC-Gal d 4 bioconjugate at 0.38 column volume (CV) or 9.1 min. The representative fluorescence spectrum taken of peak fractions confirms the presence of AuNC bioconjugate with characteristic emission at 700 nm (inset). Small peaks at >0.7 CV (denoted by *) represent leftover reagent from the bioconjugation process. No significant fluorescence was observed for these fractions.

diluted in the sample diluent buffer provided by the manufacturer to 3000 ng/mL in order to fit within the range of the standard curve (0−4000 ng/mL). Absorbance was measured using a Varioskan LUX spectrometer and compared to a standard curve to obtain the absolute protein concentration. All values were normalized to a control reaction carried out using an equivalent concentration of unmodified Gal d 4 and HEW.

For human IgE studies, a human monoclonal IgE antibody specific for hen egg lysozyme (1E7) was purified by affinity chromatography from a hybridoma cell line. The original IgE-producing human cell was isolated from a food allergic donor, using methods described in detail.[30] Samples of Gal d 4- and HEW-AuNC were lyophilized and subsequently rehydrated prior to analysis. A competitive inhibition was selected to take advantage of the anti-IgE detection methods. ELISA plates were coated overnight with 100 mg/mL lysozyme in coating buffer (50 mM carbonate/bicarbonate buffer pH 9.6). Plates were washed four times with PBS-T (PBS pH 7.4 + 0.05% Tween 20) then blocked with PBS-T/B (PBS-T + 1% bovine serum albumin). Separately, 1E7 (10 mg/mL) was mixed with serial dilutions of lysozyme (5 to 0.1 mg/mL) and incubated

https://doi.org/10.1021/acsomega.4c07425
ACS Omega 2025, 10, 9040−9050

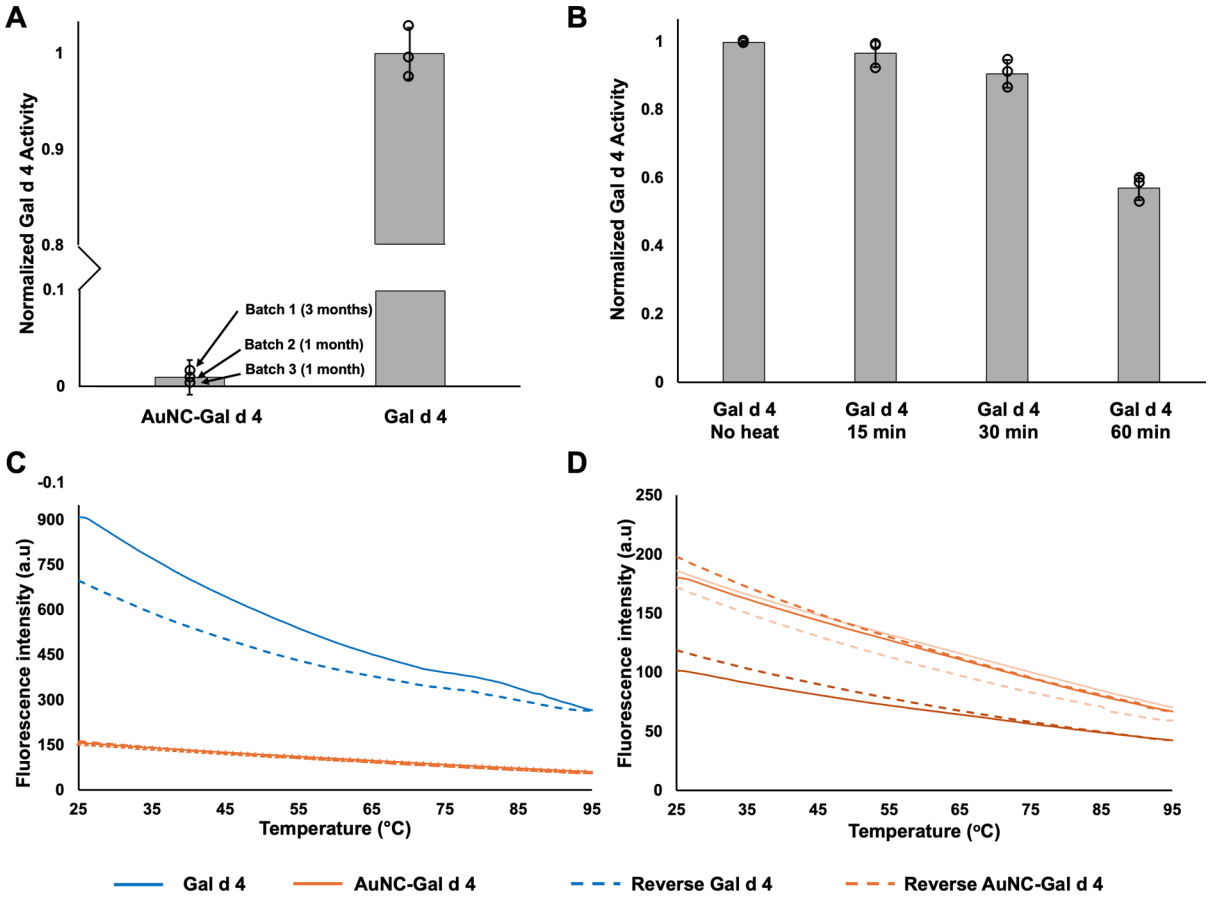

Figure 3. AuNC bioconjugation irreversibly disrupts the protein structure/function. (A) Catalytic activity of AuNC-Gal d 4 and unfunctionalized Gal d 4. The activity was assessed using an equivalent amount of protein and presented as relative (normalized) values. Three independent batches of AuNC-Gal d 4 were analyzed in triplicate (for a total of 9 trials). The average of each individual batch is shown in circles along with the age of each batch at the time of analysis. Three trials were run on unfunctionalized Gal d 4. The overall averages and standard deviations for the two conditions are shown in the bar graph. (B) Gal d 4 activity following thermal denaturation at 90 °C at different heat exposure times: 0, 15, 30, and 60 min showing both the incomplete denaturation of Gal d 4 and the rapid recovery of catalytic activity upon returning to room temperature. All Gal d 4 activity samples were allowed to cool for 10 min after heat exposure, and their values were normalized against the control sample of equivalent concentration of unconjugated Gal d 4. (C) Average thermal denaturation curves for Gal d 4 (blue) and AuNC-Gal d 4 (orange), as assessed using tryptophan fluorescence (λ_{ex}: 280 nm, λ_{em}: 340 nm). Forward (25 → 95 °C) and reverse (95 → 25 °C) melting curves are shown in solid and dashed lines, respectively. (D) A close-up view of the individual AuNC-Gal d 4 melting curves from three separate trials.

for 60 min before adding to the ELISA plate and incubating for 1 h. Detection utilized anti-IgE-HRP-conjugated Ab and 100 mL of TMB substrate. When the absorbance at 605 nm approached 1.0−1.2, the reaction was stopped with 100 mL of 1 M HCl and the absorbance at 450 nm was recorded on a SpectraMax iD3.

Hemolysis Assay. Hemocompatibility of the AuNC-Gal d 4 was tested using a hemolysis assay adapted from previous work by Murray and colleagues.[31] Sheep erythrocytes (RBC) were washed and resuspended with PBS at pH 7.2. Washed RBC (100 μL) was added to 900 μL of AuNC-Gal d 4 or Gal d 4 solutions (25−121 μM) in PBS and incubated for 30 min at room temperature. The resulting solutions were centrifuged at 2000g for 5 min, then 20 μL of the supernatant was added to 100 μL of PBS in a 96-well plate to read the absorbance at 580 nm. Values were normalized against negative (PBS) and positive (10% SDS) controls, representing 0 and 100% lysis, respectively.

RESULTS

Confirming the Physical Properties of AuNC Bioconjugates. Based on previous works, the AuNC-Gal d 4 bioconjugates display a distinct emission peak around 650−700 nm with an excitation wavelength of 360 nm.[25,32] The AuNC-Gal d 4 employed in this work produced a similar fluorescence spectrum (Figure 1A), confirming successful formation of the desired AuNC-Gal d 4 species. This is accompanied by the formation of a light-brown color under visible light, which also easily identifies the production of AuNC-Gal d 4 (Figure 1B). AuNC-Gal d 4 was further characterized by DLS and TEM. Figure 1C depicts a representative size distribution of AuNC-Gal d 4 (7.7 ± 4.5 nm) vs Gal d 4 (1.9 ± 0.4 nm) and illustrates the mean size increase of the bioconjugate compared to the native protein structure, suggesting successful protein binding on the AuNC surface. Further TEM characterization (Figure 1D) illustrates the formation of AuNC with an average core size of 2.1 ± 0.4 nm. Size distribution analysis of the imaging measurements clearly shows a rather monodisperse NC formation (Figure 1E). Elemental composition of the NC was confirmed to be Au

https://doi.org/10.1021/acsomega.4c07425
ACS Omega 2025, 10, 9040−9050

by energy-dispersive X-ray spectroscopy or EDS (Figure S5). These results confirm that we are indeed able to replicate the AuNC-Gal d 4 previously described. In the context of Allergold generation, our results provide strong evidence for a monodisperse compound with predictable and consistent physical properties. This contrasts with allergoids produced using "traditional" chemical methods, which tend to have high levels of heterogeneity.[16]

AuNC Conjugation Irreversibly Alters Lysozyme Structure/Function. Previous studies on AuNC-Gal d 4 bioconjugates show a drastic change in the secondary structure. This can be seen by a significant reduction in tryptophan fluorescence relative to the unfunctionalized Gal d 4, consistent with an increased exposure to the polar solvent (Figure 2).[32−34] This is further confirmed using circular dichroism (CD), where a loss of α-helical content and an increase in β-sheet elements were reported.[23] Treatment of Gal d 4 with NaOH alone (negative control, see Materials and Methods) resulted in the formation of a precipitate that was not observed in the AuNC-Gal d 4 bioconjugate. Nonetheless, significant tryptophan fluorescence was retained. Gal d 4 secondary structure was also unperturbed by extreme pH, suggesting that the structural perturbations observed in AuNC-Gal d 4 are a direct result of AuNC bioconjugation.

These structural perturbations were reported to diminish Gal d 4's natural enzymatic activity.[35] The AuNC-Gal d 4 generated in this work shows perturbations similar to both its structure and function (Figures 2 and 3), confirming the generation of an altered Gal d 4 state upon bioconjugation. Alterations to protein structure were further confirmed using NMR, which showed a drastic decrease in both the dispersion and intensity of the protein amide ^{1}H peaks upon AuNC bioconjugation (Figure 2B). This could potentially reflect a loss of secondary structure, although it could also be attributed to a change in protein conformational dynamics, an increase in complex size and heterogeneity, or a combination of all three factors.

Previous studies on AuNC-Gal d 4 attribute the observed structural perturbations to the formation of Au−S bonds between cysteine residues and gold. The covalent nature of these Au−S bonds is expected to afford the resulting bioconjugates a high degree of resilience. To test this conjecture, samples of AuNC-Gal d 4 were applied to an S75 size-exclusion column. AuNC-Gal d 4 eluted as a single, homogeneous peak at ∼0.4 column volumes (CV) or 110 mL, corresponding to an apparent molecular weight of 25 kDa or an apparent particle size of 2.5 nm, assuming typical density values for a globular protein. The eluted species retained the same fluorescence properties as the untreated AuNC-Gal d 4 (Figure 2E). No separate peaks for free Gal d 4 or unbound AuNC could be observed, suggesting that the Gal d 4 bioconjugates represent a stable covalent complex rather than one maintained by reversible nonspecific interactions.

The covalent nature of these Au−S linkages also affords our AuNC-Gal d 4 a significant degree of resilience to environmental degradation. This can be visualized in Figure 3, which examines the catalytic activity of AuNC-Gal d 4 following several months of storage under aqueous conditions. No recovery in enzymatic activity observed over the time period investigated. Samples of AuNC-Gal d 4 were also subjected to lyophilization and were found to retain their immunogenic properties (discussed below). This represents a clear advantage over thermally or chemically denatured versions of Gal d 4, which can either fail to fully denature and/or can be readily reversed upon removal of the denaturant due to the disulfide bonds remaining unaltered.[36] Indeed, samples of Gal d 4 subjected to thermal denaturation retained significant activity (Figure 3B). Furthermore, a drastic recovery in catalytic activity was observed upon returning the Gal d 4 samples to room temperature. This phenomenon can be better visualized by using tryptophan fluorescence measurements at increasing temperatures. Here, Gal d 4 showed a steady decrease in intrinsic tryptophan fluorescence consistent with the cooperative unfolding of a globular protein (Figure 3C).[33] However, reversing the temperature gradient resulted in a significant recovery of the fluorescence intensity. This, coupled with the gradual recovery of catalytic activity following thermal denaturation discussed above, suggests that Gal d 4 refolded or partially refolded back into its native structure within minutes. In contrast, AuNC-Gal d 4 tryptophan fluorescence did not change significantly upon heating. Furthermore, no significant recovery in tryptophan fluorescence was observed upon reversing the temperature gradient as shown in Figure 3C. These results confirm that our AuNC Allergold is able to not only disrupt the structure of its conjugated allergens but also maintain this altered state over a range of conditions. Such behavior is in stark contrast to unfunctionalized Gal d 4 and suggests the potential utility of Allergolds as an alternative to traditional approaches

Biocompatibility of AuNC-Gal d 4. One of the advantages of our approach to hypoallergen generation is the high level of biocompatibility generally observed for AuNC bioconjugates, a key consideration given its potential applications as an AIT agent. To confirm that the AuNC-Gal d 4 conjugates produced in this study conform to the expected biocompatibility, we conducted a hemolysis assay using mammalian (sheep) red blood cells (RBC). The resultant data are shown in Table 1. Neither AuNC-Gal d 4 nor Gal d 4 differed significantly from the negative control across range concentrations tested.

Table 1. Hemolysis Assay Results of AuNC-Gal d 4 and Gal d 4[a]

sample	concentration (μM)	normalized lysis (%)
negative control		0.00 ± 1.66
positive control		100.00 ± 20.38
AuNC-Gal d 4	25	1.00 ± 2.61
	50	4.24 ± 6.79
	75	0.10 ± 0.57
	121	3.78 ± 3.57
Gal d 4	25	1.67 ± 2.28
	50	−0.41 ± 0.16
	75	0.88 ± 2.65
	121	1.72 ± 2.11

[a]Values are normalized against a PBS negative control (0% lysis) and 10% SDS positive control (100% lysis). No statistically significant differences were observed between the AuNC-Gal d 4/Gal d 4 samples and the negative control.

AuNC-Based Allergolds Disrupt Antibody Binding. The perturbations to the Gal d 4 structure upon AuNC bioconjugation are expected to disrupt antibody binding. To assess this hypothesis, commercially available ELISA were used to measure antibody (IgG) binding of Gal d 4 and AuNC-Gal d 4. The results were normalized with respect to a Gal d 4

https://doi.org/10.1021/acsomega.4c07425
ACS Omega 2025, 10, 9040−9050

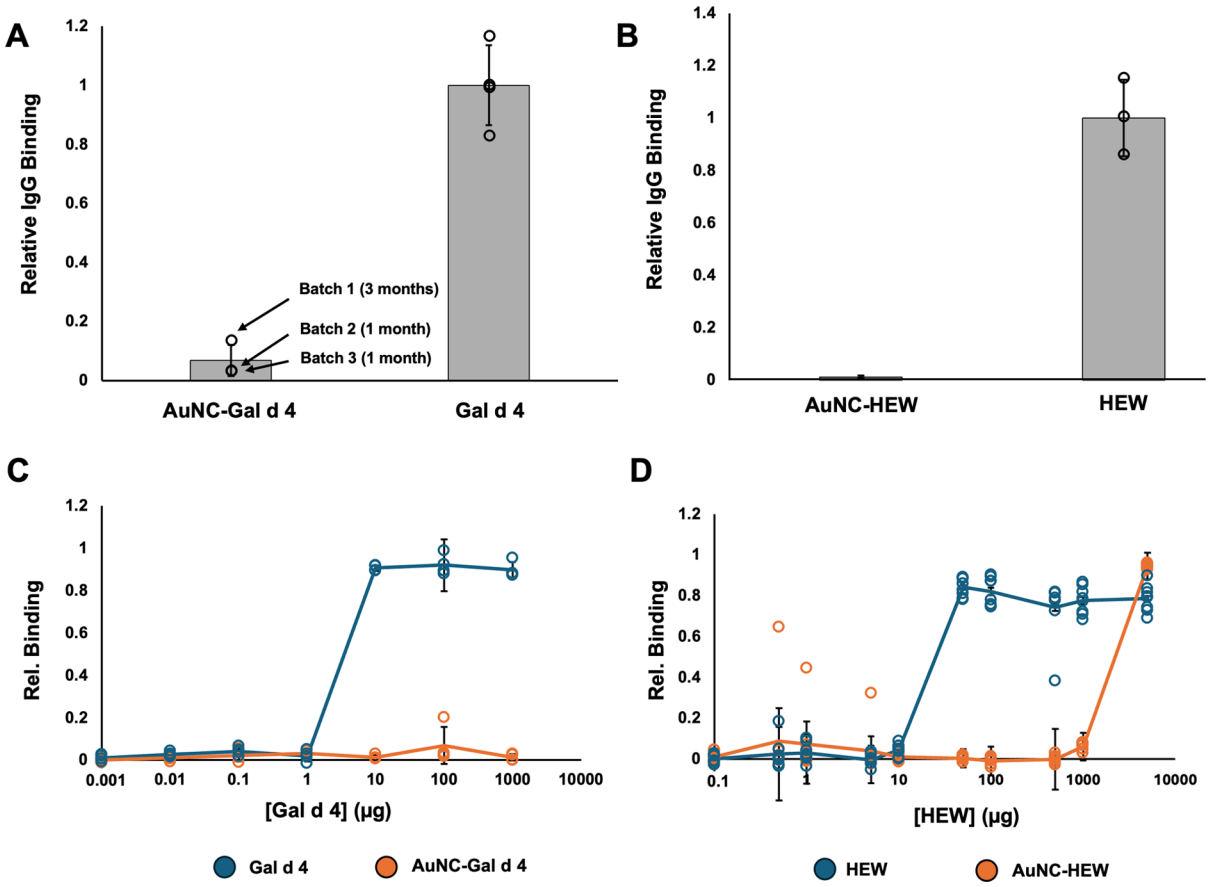

Figure 4. Allergolds display reduced antibody binding. (A) Average relative IgG binding of three different batches of prepared AuNC-Gal d 4 vs a Gal d 4 control determined by ELISA. Each AuNC-Gal d 4 batch was analyzed three times (for a total of 9 trials). The average of each individual batch is shown in circles, along with the age of each batch at the time of analysis is shown. Note that the values from batch 2 and batch 3 overlap. Four trials were run on the unfunctionalized Gal d 4, and the individual results are shown in circles. The overall averages and standard deviations for the two conditions are shown in the bar graph. (B) Relative IgG binding of prepared AuNC-HEW vs a HEW control. Average and standard deviations for all trials are shown. Individual results for AuNC-HEW overlap and are omitted for clarity. All IgG ELISA were carried out using 3000 ng/mL analyte. (C) Competitive inhibition-ELISA assay examining the binding capability of unfunctionalized and AuNC-Gal d 4 against human IgE's from allergic patients. This assay measures the ability of the analyte to compete with a fixed concentration of Gal d 4 for IgE binding (Materials and Methods). (D) The ability of HEW and AuNC-HEW to bind IgE. Data from the individual repeats (minimum 3) are shown in circles.

control containing an equivalent amount of allergen and expressed as relative IgG binding (Figure 4A). AuNC-Gal d 4 showed a significant reduction in binding, consistent with the proposed hypothesis. The extreme resilience discussed in previous sections also extended to antibody binding, with no recovery of IgG activity following several months of storage under aqueous conditions.

To confirm the utility of AuNC-Gal d 4 under potentially therapeutic conditions, we examined their ability to bind human IgE derived from allergic patients. Using a competitive inhibition ELISA, the AuNC-Gal d 4 Allergold and unfunctionalized Gal d 4 allergen was assessed for their ability to block the 1E7 antibody from binding immobilized Gal d 4. Gal d 4 was able to successfully block binding, indicating a strong interaction with 1E7. The blocking capability of AuNC-Gal d 4 was significantly reduced with a ≥100-fold reduction in IgE binding (Figure 4C). It should be noted that these samples were subjected to lyophilization prior to testing (see Materials and Methods). Their ability to retain Gal d 4 in a hypoallergenic state following lyophilization provides further evidence for their long-term stability, a key requirement for use in a clinical setting.

Allergolds as a Versatile Platform for Hypoallergen Production. Literature precedent suggests that the formation of the AuNC-Gal d 4 bioconjugate is mediated by gold−sulfur linkages involving cysteine residues.[22] The relatively non-specific nature of this interaction suggests that the AuNC-bioconjugation strategy described herein could be easily adapted to other allergenic protein systems. To test this hypothesis, ovalbumin (Gal d 2)-functionalized AuNC were examined. Gal d 2 nanoclusters have been described previously, though as with Gal d 4, the potential applications of these nanoclusters for AIT were not explored.[37] While Gal d 2 contains proportionally fewer cysteine residues (1.6%) than Gal d 4 (6.1%), a notable decrease in secondary structure was still observed in these works.[37] Fluorescence emission spectroscopy (λ_{ex}: 365 nm) indicates that we were able to successfully replicate the AuNC-Gal d 2 bioconjugate (Figure 5A) with an emission peak at 700 nm and formation of a characteristic orange-pink AuNC (Figure 5B). AuNC formation significantly decreased intrinsic tryptophan fluorescence (Figure 5C) similar to what was observed for its AuNC-Gal d 4 counterpart, suggesting a loss of protein structure. Further analysis of these structural changes via CD confirms a

https://doi.org/10.1021/acsomega.4c07425
ACS Omega 2025, 10, 9040−9050

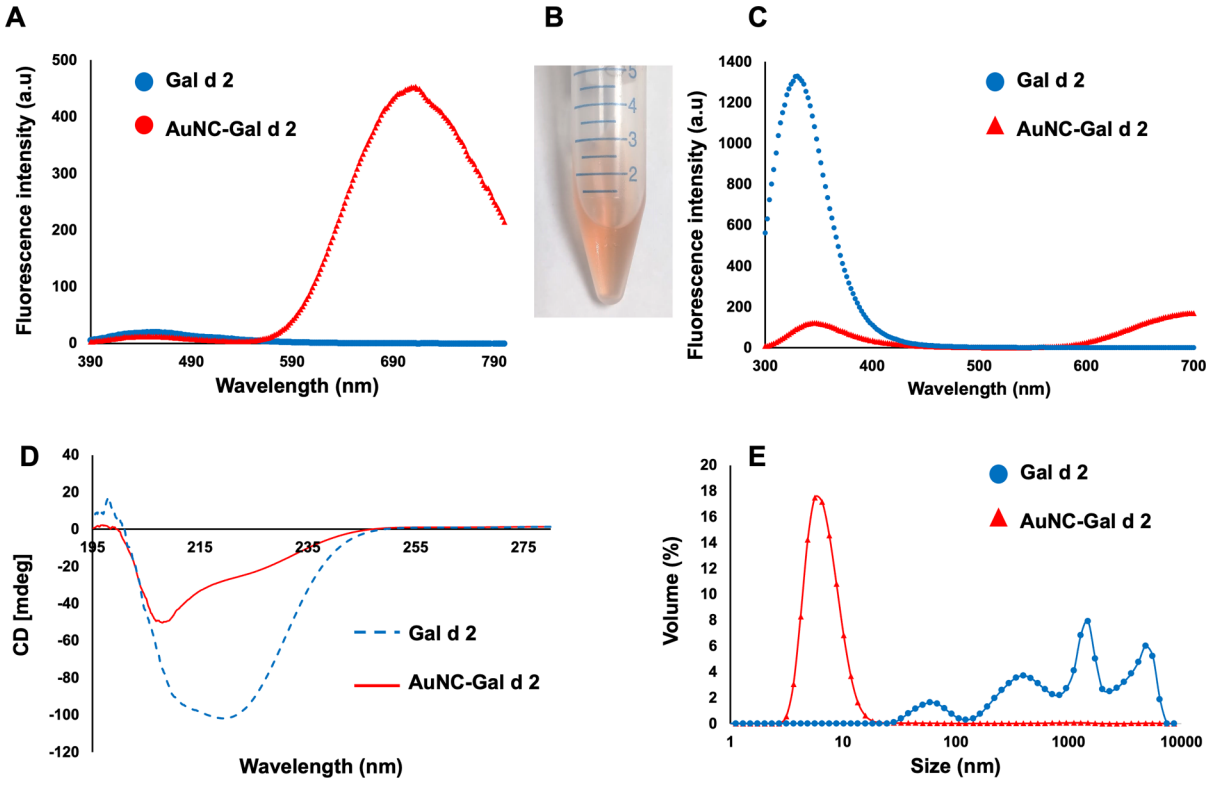

Figure 5. Impact of Allergold formation on Gal d 2 structure and morphology. (A) Average fluorescence emission spectra (λ_{ex}: 365 nm) of prepared AuNC-Gal d 2 and aqueous solution of 0.180 mM Gal d 2. (B) Representative AuNC-Gal 2 under visible light. (C) Average fluorescence emission spectra (λ_{ex}: 280 nm) of prepared AuNC-Gal d 2 and aqueous solution of 0.180 mM Gal d 2. (D) Average CD spectra of prepared AuNC-Gal d 2 and aqueous Gal d 2 solution. (E) Average DLS size distribution per volume plot of prepared AuNC-Gal d 2 and aqueous solution of 0.180 mM Gal d 2.

marked loss of α-helical secondary structure (Figure 5D), though not to the same extent as was observed for Gal d 4 upon AuNC conjugation, potentially reflecting the lower cysteine content of Gal d 2 affording diminished gold−sulfur interactions.

In addition to the reduced cysteine content, Gal d 2 is much more hydrophobic than Gal d 4 and has the capacity to self-assemble into fibrillar aggregates.[38,39] This can be visualized using DLS. Here, Gal d 2 showed a wide distribution of sizes (Figure 5E), with some complexes reaching >10 μm with a mean size of 1510 ± 837 nm and poor solubility. Upon conjugation with gold, Gal d 2 transforms into a homogeneous mixture with a mean particle size of 7.6 ± 2.1 nm and good water solubility similar to AuNC-Gal d 4. The ability to generate a consistent, well-defined product with good water solubility further enhances the potential for AuNC-based Allergolds as agents for AIT treatments.

An additional advantage of our AuNC Allergolds is their ability to be produced using a native (unaltered) allergen. This, combined with the relatively mild conditions under which AuNC formation is observed, raises the possibility that hypoallergenic AuNC conjugates can be generated from whole protein extracts, significantly reducing the barrier to AIT generation and therapeutic development. To test this hypothesis, whole hen egg whites (HEW) were used to prepare AuNC bioconjugates. Since Gal d 4 accounts for an estimated 3.5% of all proteins in the HEW mixture, anti-Gal d 4 antibodies displayed significant binding to the unmodified HEW control (Figure 4B).[40] Conjugating HEW with AuNC significantly reduced both IgG and IgE antibody binding, similar to what was observed in the AuNC-Gal d 4 bioconjugate, verifying the hypoallergenic properties of AuNC produced from crude protein extracts.

It should be noted that HEW is a heterogeneous mixture containing several other allergens including Gal d 2 (54%) and ovomucoid (Gal d 1, 11%). Thus, AuNC bioconjugation represents a convenient method to generate hypoallergens for a vast array of food allergens simultaneously from crude protein extracts.

DISCUSSION

The results presented in this work illustrate the potential of AuNC-based bioconjugates to reduce the level of antibody binding to food allergens. These Allergolds are uniform and monodisperse with predictable physical and chemical properties, high biocompatibility, and elevated resilience under a range of conditions. This contrasts with traditional allergoids generated by using chemical cross-linking agents such as formaldehyde or glutaraldehyde. While quick and effective, the nonspecific nature of these agents tends to result in the formation of dimers, oligomers, and higher-order aggregates, with one study on birch pollen allergoids showing a size distribution range from 6.5 to 200 kDa following glutaraldehyde treatment.[16] The heterogeneous nature of these mixtures complicates efforts to precisely define allergen content and control IgE reactivity, necessitating special requirements for quality control.[16−18] The nonspecific nature of these chemical cross-linkers also makes them potentially toxic, necessitating strict quality control measures to ensure complete removal of these compounds prior to administration.

https://doi.org/10.1021/acsomega.4c07425
ACS Omega 2025, 10, 9040−9050

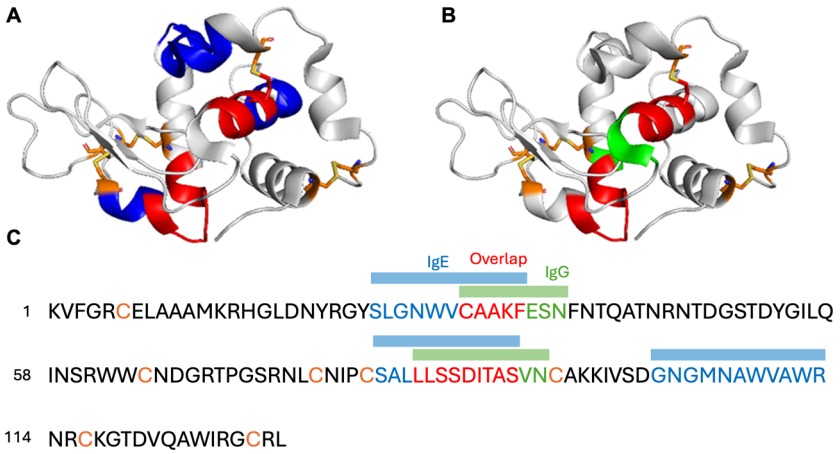

Figure 6. Comparison of known Gal d 4 IgG and IgE epitopes. X-ray crustal structure of Gal d 4 (PDB: 1dpx) showing dominant (A) IgE binding epitopes in blue and (B) IgG epitopes in green. In both images, cysteine residues are shown in orange, while residues common to both IgE and IgG (AA 31−34 and AA 84−91) are shown in red. (C) IgE and IgG epitopes are displayed on the Gal d 4 sequence.

In some cases, AuNC can even enhance the physical properties of the native allergen itself, as seen in the case of Gal d 2. Here, Allergold formation enhanced the solubility and eliminated the presence of higher-order aggregates. Related to this is the observed ability of certain allergens (including both Gal d 2 and Gal d 4) to self-assemble into heterogeneous aggregates, further complicating efforts to control dosages and induce a predictable immunological response.[41] Indeed, Gal d 4 is often used as a model system to study amyloid fibril formation.[42] Here, fibril formation is triggered by a reduction of structural disulfides coupled with the addition of denaturants, such as ethanol, as might be expected in traditional allergoid formulations. This results in the formation of a β-sheet intermediate, perhaps mirroring the structural perturbations observed upon AuNC-bioconjugation. Despite this, no amyloid fibril formation was observed in our Gal d 4 Allergolds, demonstrating their utility over traditional approaches. The resilience of AuNC-based Allergolds also prevents recovery of the native allergen structure, as has been observed for the thermally denatured Gal d 4 seen in this work, and in studies on both Gal d 4 and other allergens reported elsewhere.[43,44] Even chemically produced allergoids are susceptible to degradation under similar conditions,[45] though the stability of our Allergolds remains to be systematically evaluated in a similar manner. In addition to being extremely resilient, the Au−S bond offers additional advantages. By leveraging the prevalence of disulfide bonds among allergenic proteins, AuNC bioconjugation can be rapidly adapted to generate Allergolds from other allergens such as Gal d 2 and HEW bioconjugates as shown in this work or any of the hundreds of other protein-AuNC's described in the literature.

The ability of Allergolds to retain Gal d 4 in a denatured state under physiological conditions resulted in an ≥100-fold reduction in IgE binding. While additional experiments are required to assess their effectiveness in a clinical setting, it is worth considering the fact that chemically cross-linked Gal d 4 allergoids displayed similar reductions in IgG/IgE binding as our AuNC-Gal d 4 bioconjugates,[44] indicating that the latter are at least capable of matching the performance of more traditional formulations. Curiously, this same work found that physical denaturants such as urea and heat had little or no impact on Gal d 4 immunogenicity, potentially reflecting the reversibility of Gal d 4 denaturation discussed above.[44] It is worth noting that not all food allergens show the same reversible denaturation properties as Gal d 4. In these cases, irreversible denaturation by physical methods such as heat or pH can reduce IgE/IgG binding to a similar degree as AuNC bioconjugation.[46,47] This positions Allergolds as a novel tool, which, in concert with other techniques, provide an expansive "toolbox" through which we can generate denatured/destabilized versions of allergenic proteins

Despite their established use in AIT, the specific mechanisms through which these denatured and destabilized allergen species are able to induce a protective IgG response are still a matter of scientific debate. This work does not aim to provide a comprehensive exploration of the topic. However, the ability to maintain the allergen in a denatured state is recognized as being key to the process. The known IgE epitopes centered on the structure regions of Gal d 4, making them susceptible to disruption by AuNC conjugation. It should also be noted that there is substantial overlap between the dominant binding epitopes of both IgE and IgG antibodies (Figure 6),[48] consistent with the similar levels of inhibition observed in both antibodies. This phenomenon is common to many allergen systems; in fact, a decrease in IgG binding is a sufficient quality control for most allergoids, owing to the difficulty in obtaining IgE antibodies.[16]

AuNC bioconjugates have received significant attention in recent years due to their ability to alter the structure and function of their conjugated proteins. In this work, we show that this property can be leveraged to generate conjugates with reduced antibody binding from native (unaltered) food allergens and whole egg whites. The resulting "Allergolds" were found to be extremely stable with no recovery in protein structure or antibody binding, highly consistent, and extremely biocompatible. While AuNC-based Allergolds have yet to be tested in vivo, these favorable properties make them a compelling alternative to both "traditional" allergoid formulations and emerging "precision-engineered" approaches.

■ ASSOCIATED CONTENT

Data Availability Statement

The antibody binding data (Figure 4), hemolysis data (Table 1), and Gal d 2 structural data (Figure 5) are not publicly available as they represent unpublished data for future publications and patents but can be provided by the

https://doi.org/10.1021/acsomega.4c07425
ACS Omega 2025, 10, 9040−9050

corresponding author upon reasonable request. All other data underlying this study is available via the St. Francis Xavier University Online Data Repository (Borealis) at 10.5683/SP3/T8GKYW.

Supporting Information

The Supporting Information is available free of charge at https://pubs.acs.org/doi/10.1021/acsomega.4c07425.

Additional biophysical characterization of AuNC-Gal d 4 bioconjugates: Figures S1−S4: Additional TEM images of AuNC-Gal d 4 bioconjugates; Figure S5: Energy-dispersive spectroscopy (EDS) spectra confirming the presence of gold in the nanoclusters (PDF)

AUTHOR INFORMATION

Corresponding Author

Alexander C.Y. Foo − *Dept. of Chemistry, St. Francis Xavier University, Antigonish, NS B2G 2W5, Canada;* orcid.org/0000-0002-4331-2085; Email: afoo@stfx.ca

Authors

Victor Martinez-Macias − *Dept. of Chemistry, St. Francis Xavier University, Antigonish, NS B2G 2W5, Canada*

Scott A. Gabel − *Genome Integrity and Structural Biology Laboratory, National Institute of Environmental Health Sciences, Research Triangle Park, North Carolina 27709, United States*

J. Craig Bennett − *Dept. of Physics, Acadia University, Wolfville, NS B4P 2R6, Canada;* orcid.org/0000-0003-3122-6486

Scott A. Smith − *Dept. of Pathology, Microbiology, and Immunology, Vanderbilt University Medical Center, Nashville, Tennessee 37232, United States*

Geoffrey A. Mueller − *Genome Integrity and Structural Biology Laboratory, National Institute of Environmental Health Sciences, Research Triangle Park, North Carolina 27709, United States;* orcid.org/0000-0001-8361-5323

Geniece L. Hallett-Tapley − *Dept. of Chemistry, St. Francis Xavier University, Antigonish, NS B2G 2W5, Canada*

Complete contact information is available at: https://pubs.acs.org/10.1021/acsomega.4c07425

Author Contributions

§G.L.H.-T. and A.C.Y.F. contributed equally to this work.

Funding

This work was supported by a Natural Science and Engineering Research Council (NSERC) Discovery Grant and Discovery Launch Supplement (RGPIN-2023-03474, DGECR-2023-00224) to A.C.Y.F., a Discovery Grant to J.C.B. (RGPIN-2017-04372), and a Discovery Grant to G.L.H.-T. (RGPIN-2022-03967). V.M.-M. was supported with a Research Nova Scotia - Scotia Scholars Award (no. 2024-3098) and a J.P Cunningham Internship. G.A.M was supported by the Intramural Program of the National Institute of Environmental Health Sciences, (ZIA-ES102906). S.A.S. was supported by the NIH/National Institute of Allergy and Infectious Disease (R01AI155668 and R21AI123307).

Notes

The authors declare no competing financial interest.

ACKNOWLEDGMENTS

We would like to thank Dr. Robert Petrovich (NIEHS) for his technical assistance with the circular dichroism (CD) experiments. We would also like to thank StFX University Building Opportunities for Learning and Development (BOLD) Program (with support from the Department of Labour, Skills, Immigration, Government of Nova Scotia) for the support they provided to V.M.-M. during this project, and the other funding agencies described below.

REFERENCES

(1) McWilliam, V. L.; Koplin, J. J.; Field, M. J.; Sasaki, M.; Dharmage, S. C.; Tang, M. L. K.; Sawyer, S. M.; Peters, R. L.; Allen, K. J. Self-Reported Adverse Food Reactions and Anaphylaxis in the SchoolNuts Study: A Population-Based Study of Adolescents. *J. Allergy Clin. Immunol.* **2018**, *141* (3), 982−990.

(2) Umasunthar, T.; Leonardi-Bee, J.; Turner, P. J.; Hodes, M.; Gore, C.; Warner, J. O.; Boyle, R. J. Incidence of Food Anaphylaxis in People with Food Allergy: A Systematic Review and Meta-analysis. *Clin. Exp. Allergy* **2015**, *45* (11), 1621−1636.

(3) Thomas, N. M. Racial and Ethnic Data Reported for Peanut Allergy Epidemiology Do Little to Advance Its Cause, Treatment, or Prevention. *Front. Public Health* **2021**, *9*, No. 685240.

(4) Jafri, S.; Frykas, T. L.; Bingemann, T.; Phipatanakul, W.; Bartnikas, L. M.; Protudjer, J. L. P. Food Allergy, Eating Disorders and Body Image. *J. Affect. Disord. Rep.* **2021**, *6*, No. 100197.

(5) De Blok, B. M. J.; Vlieg-Boerstra, B. J.; Oude Elberink, J. N. G.; Duiverman, E. J.; DunnGalvin, A.; Hourihane, J. O.; Cornelisse-Vermaat, J. R.; Frewer, L.; Mills, C.; Dubois, A. E. J. A Framework for Measuring the Social Impact of Food Allergy across Europe: A EuroPrevall State of the Art Paper. *Allergy* **2007**, *62* (7), 733−737.

(6) Wu, A. Y.-Y. Immunotherapy - Vaccines for Allergic Diseases. *J. Thorac. Dis.* **2012**, *4*, 198.

(7) Durham, S. R.; Shamji, M. H. Allergen Immunotherapy: Past, Present and Future. *Nat. Rev. Immunol.* **2023**, *23* (5), 317−328.

(8) Pavón-Romero, G. F.; Parra-Vargas, M. I.; Ramírez-Jiménez, F.; Melgoza-Ruiz, E.; Serrano-Pérez, N. H.; Teran, L. M. Allergen Immunotherapy: Current and Future Trends. *Cells* **2022**, *11* (2), 212.

(9) Turkalj, M.; Miletić Gospić, A.; Višekruna Džidić, I.; Banić, I. Food Allergen Immunotherapy in the Treatment of Patients with IgE-Mediated Food Allergy. *Medicina (Mex.)* **2024**, *60* (1), 121.

(10) Marsh, D. G.; Lichtenstein, L. M.; Campbell, D. H. Studies on allergoids' prepared from naturally occurring allergens. *Immunology* **1970**, *18* (5), 705−722.

(11) Marsh, D. G.; Norman, P. S.; Roebber, M.; Lichtenstein, L. M. Studies on Allergoids from Naturally Occurring Allergens III. Preparation of Ragweed Pollen Allergoids by Aldehyde Modification in Two Steps. *J. Allergy Clin. Immunol.* **1981**, *68* (6), 449−459.

(12) Haddad, Z. H.; Marsh, D. G.; Campbell, D. H. Studies on "Allergoids" Prepared from Naturally Occurring Allergens II. Evaluation of Allergenicity and Assay of Antigenicity of Formalinized Mixed Grass Pollen Extracts. *J. Allergy Clin. Immunol.* **1972**, *49* (4), 197−209.

(13) Jiménez-Saiz, R.; Rupa, P.; Mine, Y. Immunomodulatory Effects of Heated Ovomucoid-Depleted Egg White in a BALB/c Mouse Model of Egg Allergy. *J. Agric. Food Chem.* **2011**, *59* (24), 13195−13202.

(14) Wai, C. Y. Y.; Leung, N. Y. H.; Leung, P. S. C.; Chu, K. H. Immunotherapy of Food Allergy: A Comprehensive Review. *Clin. Rev. Allergy Immunol.* **2019**, *57* (1), 55−73.

(15) Carnes, J.; Gallego, M. T.; Moya, R.; Iraola, V. Allergoids for Allergy Treatment. *Recent Pat. Inflamm. Allergy Drug Discovery* **2018**, *12* (2), 110−119.

(16) Zimmer, J.; Bonertz, A.; Vieths, S. Quality Requirements for Allergen Extracts and Allergoids for Allergen Immunotherapy. *Allergol. Immunopathol. (Madr.)* **2017**, *45*, 4−11.

(17) Starchenka, S.; Bell, A. J.; Mwange, J.; Skinner, M. A.; Heath, M. D. Molecular Fingerprinting of Complex Grass Allergoids: Size Assessments Reveal New Insights in Epitope Repertoires and Functional Capacities. *World Allergy Organ. J.* **2017**, *10*, 17.
(18) Gil, M. V.; Fernández-Rivera, N.; Pastor-Vargas, C.; Cintas, P. Food Allergens: When Friends Become Foes—Caveats and Opportunities for Oral Immunotherapy Based on Deactivation Methods. *Nutrients* **2023**, *15* (16), 3650.
(19) Min, J.; Keswani, T.; LaHood, N. A.; Lytle, I. R.; Marini-Rapoport, O.; Andrieux, L.; Sneed, S. L.; Edwards, L. L.; Petrovich, R. M.; Perera, L.; Pomés, A.; Pedersen, L. C.; Patil, S. U.; Mueller, G. A. Design of an Ara h 2 Hypoallergen from Conformational Epitopes. *Clin. Exp. Allergy* **2024**, *54* (1), 46−55.
(20) Mine, Y.; Sasaki, E.; Zhang, J. W. Reduction of Antigenicity and Allergenicity of Genetically Modified Egg White Allergen, Ovomucoid Third Domain. *Biochem. Biophys. Res. Commun.* **2003**, *302* (1), 133−137.
(21) Ghosh, D.; Baksi, A.; Mudedla, S. K.; Nag, A.; Ganayee, M. A.; Subramanian, V.; Pradeep, T. Gold-Induced Unfolding of Lysozyme: Toward the Formation of Luminescent Clusters. *J. Phys. Chem. C* **2017**, *121* (24), 13335−13344.
(22) Xu, Y.; Sherwood, J.; Qin, Y.; Crowley, D.; Bonizzoni, M.; Bao, Y. The Role of Protein Characteristics in the Formation and Fluorescence of Au Nanoclusters. *Nanoscale* **2014**, *6* (3), 1515−1524.
(23) Russell, B. A.; Jachimska, B.; Komorek, P.; Mulheran, P. A.; Chen, Y. Lysozyme Encapsulated Gold Nanoclusters: Effects of Cluster Synthesis on Natural Protein Characteristics. *Phys. Chem. Chem. Phys.* **2017**, *19* (10), 7228−7235.
(24) Xie, J.; Zheng, Y.; Ying, J. Y. Protein-Directed Synthesis of Highly Fluorescent Gold Nanoclusters. *J. Am. Chem. Soc.* **2009**, *131* (3), 888−889.
(25) Wei, H.; Wang, Z.; Yang, L.; Tian, S.; Hou, C.; Lu, Y. Lysozyme-Stabilized Gold Fluorescent Cluster: Synthesis and Application as Hg2+ Sensor. *Analyst* **2010**, *135* (6), 1406.
(26) Joseph, D.; Geckeler, K. E. Synthesis of Highly Fluorescent Gold Nanoclusters Using Egg White Proteins. *Colloids Surf. B Biointerfaces* **2014**, *115*, 46−50.
(27) Li, M.; Zhu, N.; Zhu, W.; Zhang, S.; Li, F.; Wu, P.; Li, X. Enhanced Emission and Higher Stability Ovalbumin-Stabilized Gold Nanoclusters (OVA-AuNCs) Modified by Polyethyleneimine for the Fluorescence Detection of Tetracyclines. *Microchem. J.* **2021**, *169*, No. 106560.
(28) Micsonai, A.; Wien, F.; Kernya, L.; Lee, Y.-H.; Goto, Y.; Réfrégiers, M.; Kardos, J. Accurate Secondary Structure Prediction and Fold Recognition for Circular Dichroism Spectroscopy. *Proc. Natl. Acad. Sci. U. S. A.* **2015**, *112* (24), No. E3095.
(29) Micsonai, A.; Moussong, É.; Wien, F.; Boros, E.; Vadászi, H.; Murvai, N.; Lee, Y.-H.; Molnár, T.; Réfrégiers, M.; Goto, Y.; Tantos, Á.; Kardos, J. BeStSel: Webserver for Secondary Structure and Fold Prediction for Protein CD Spectroscopy. *Nucleic Acids Res.* **2022**, *50* (W1), W90−W98.
(30) Wurth, M. A.; Hadadianpour, A.; Horvath, D. J.; Daniel, J.; Bogdan, O.; Goleniewska, K.; Pomés, A.; Hamilton, R. G.; Peebles, R. S.; Smith, S. A. Human IgE mAbs Define Variability in Commercial Aspergillus Extract Allergen Composition. *JCI Insight* **2018**, *3* (20), No. e123387.
(31) Murray, A.; Congdon, T. R.; Tomás, R. M. F.; Kilbride, P.; Gibson, M. I. Red Blood Cell Cryopreservation with Minimal Post-Thaw Lysis Enabled by a Synergistic Combination of a Cryoprotecting Polyampholyte with DMSO/Trehalose. *Biomacromolecules* **2022**, *23* (2), 467−477.
(32) Baksi, A.; Xavier, P. L.; Chaudhari, K.; Goswami, N.; Pal, S. K.; Pradeep, T. Protein-Encapsulated Gold Cluster Aggregates: The Case of Lysozyme. *Nanoscale* **2013**, *5* (5), 2009.
(33) Moon, C. P.; Fleming, K. G. Using Tryptophan Fluorescence to Measure the Stability of Membrane Proteins Folded in Liposomes. *Methods in Enzymology; Elsevier* **2011**, *492*, 189−211.
(34) Blumlein, A.; McManus, J. J. Reversible and Non-Reversible Thermal Denaturation of Lysozyme with Varying pH at Low Ionic Strength. *Biochim. Biophys. Acta BBA - Proteins Proteomics* **2013**, *1834* (10), 2064−2070.
(35) Rigos, C. F.; Santos, H. D. L.; Thedei, G.; Ward, R. J.; Ciancaglini, P. Influence of Enzyme Conformational Changes on Catalytic Activity Investigated by Circular Dichroism Spectroscopy. *Biochem. Mol. Biol. Educ.* **2003**, *31* (5), 329−332.
(36) Kumar, S.; Kumar, T. K. S. Is Refolding of Lysozyme Template-Driven. *Biophys. J.* **2014**, *106* (2), 470a.
(37) Yang, Y.; Zhang, Y.; Thakur, A.; Li, R.; Xu, H.; Wang, Z.; Ghavami, M.; Tu, Z.; Liu, H. One-Pot Synthesis and Characterization of Ovalbumin-Conjugated Gold Nanoparticles: A Comparative Study of Adjuvanticity against the Physical Mixture of Ovalbumin and Gold Nanoparticles. *Int. J. Pharm.* **2019**, *571*, No. 118704.
(38) Kalapothakis, J. M. D.; Morris, R. J.; Szavits-Nossan, J.; Eden, K.; Covill, S.; Tabor, S.; Gillam, J.; Barran, P. E.; Allen, R. J.; MacPhee, C. E. A Kinetic Study of Ovalbumin Fibril Formation: The Importance of Fragmentation and End-Joining. *Biophys. J.* **2015**, *108* (9), 2300−2311.
(39) Weijers, M.; Barneveld, P. A.; Cohen Stuart, M. A.; Visschers, R. W. Heat-induced Denaturation and Aggregation of Ovalbumin at Neutral pH Described by Irreversible First-order Kinetics. *Protein Sci.* **2003**, *12* (12), 2693−2703.
(40) Li, Z.; Huang, X.; Tang, Q.; Ma, M.; Jin, Y.; Sheng, L. Functional Properties and Extraction Techniques of Chicken Egg White Proteins. *Foods* **2022**, *11* (16), 2434.
(41) Pérez-Tavarez, R.; Castellanos, M.; Loli-Ausejo, D.; Pedrosa, M.; Hurtado, J. L.; Rodriguez-Pérez, R.; Gasset, M. Distinct Animal Food Allergens Form IgE-Binding Amyloids. *Allergies* **2021**, *1* (1), 22−32.
(42) Cao, A.; Hu, D.; Lai, L. Formation of Amyloid Fibrils from Fully Reduced Hen Egg White Lysozyme. *Protein Sci.* **2004**, *13* (2), 319−324.
(43) Johansen, P.; Senti, G.; Martínez Gómez, J. M.; Wüthrich, B.; Bot, A.; Kündig, T. M. Heat Denaturation, a Simple Method to Improve the Immunotherapeutic Potential of Allergens. *Eur. J. Immunol.* **2005**, *35* (12), 3591−3598.
(44) Mine, Y.; Zhang, J. W. Comparative Studies on Antigenicity and Allergenicity of Native and Denatured Egg White Proteins. *J. Agric. Food Chem.* **2002**, *50* (9), 2679−2683.
(45) Manzano, A. I.; Javier Cañada, F.; Cases, B.; Sirvent, S.; Soria, I.; Palomares, O.; Fernández-Caldas, E.; Casanovas, M.; Jiménez-Barbero, J.; Subiza, J. L. Structural Studies of Novel Glycoconjugates from Polymerized Allergens (Allergoids) and Mannans as Allergy Vaccines. *Glycoconj. J.* **2016**, *33* (1), 93−101.
(46) Bloom, K. A.; Huang, F. R.; Bencharitiwong, R.; Bardina, L.; Ross, A.; Sampson, H. A.; Nowak-Węgrzyn, A. Effect of Heat Treatment on Milk and Egg Proteins Allergenicity. *Pediatr. Allergy Immunol.* **2014**, *25* (8), 740−746.
(47) Geng, Q.; Zhou, W.; Zhang, Y.; Wu, Z.; Chen, H. Effect of pH-Shift Treatment on IgE-Binding Capacity and Conformational Structures of Peanut Protein. *Foods* **2024**, *13* (21), 3467.
(48) Wang, Q.; Ju, D.; Gao, J.; Tong, P.; Chen, H. Epitope Mapping of Lysozyme Using the Chinese Egg-Allergic Sera at Both Pooled and Individual Levels. *J. Agric. Food Chem.* **2023**, *71* (16), 6458−6467.

https://doi.org/10.1021/acsomega.4c07425
ACS Omega 2025, 10, 9040−9050